Chemical Engineering Science Vol. 40, No. 5, pp. 723–731, 1985
Printed in Great Britain.

0009–2509/85 $3.00 + .00

A DYNAMIC SIMULATION OF PARTICLE DEPOSITION ON SPHERICAL COLLECTORS

MICHAEL H. PETERS,* RAMESH K. JALAN and DINESH GUPTA
Department of Chemical Engineering and Environmental Engineering, Rensselaer Polytechnic Institute, Troy, NY 12181, U.S.A.

Abstract—In the present study a greatly simplified method is outlined for the prediction of the transient behavior of particle deposition on a spherical collector, taking into consideration a variety of force terms, such as inertial, electrostatic, drag, and gravitational forces. The technique developed, which utilizes the stochastic simulation procedure of Tien *et al.*[10], is based on the concept of discretizing the fluid control volume into small cubical elements of the same size as the particles. This allows for a ready determination of both primary collection (particle deposition on the collecting sphere) and secondary collection (particle deposition on previously deposited particles). The aerosol dynamic simulations are used to study the important phenomena of the charge neutralization of a collecting sphere by the deposition of oppositely charged particles. The methodology given may be of interest in the study of particle filtration and particle coating processes.

INTRODUCTION

The deposition of aerosol particles on collecting surfaces is an important, practical problem with numerous applications including, for example, deep-bed filtration, particle agglomeration, and particle coating processes. These problems are complex, since they involve both the large-scale, macro-movements of the particle-laden fluid, as well as the smaller-scale, micro-phenomena of particle deposition (see, e.g. [1, 2]). In general, both aspects involve approximating assumptions which are necessary for a complete solution to the problem. In the macro-scale, for example, such approximations may involve estimates of the magnitudes of turbulence scales and dispersion phenomena[3]. Simplifying assumptions in the micro-scale analysis are typically the neglect of so-called particle "bounce-off" effects, particle–particle interactions, and particle re-entrainment phenomena[4].

Although it is difficult to generalize which aspect of the problem is more important, it is not uncommon for the micro-scale analysis to be in error by an order of magnitude or greater[5]. For example, in fixed-bed filtration, the so-called single collector, or target, efficiency is determined using the particle trajectories predicted from a force balance on the particle[6]. It is generally assumed that when the particle intercepts the collector boundary (sphere or cylinder) it remains there indefinitely. Furthermore, the attached particles are often assumed not to affect the deposition of later arriving particles. Although these results may give valuable insight into the behavior during the initial periods of deposition when the collecting solids are clean, they may not be accurate over the entire operating period of the deposition process [7].

*Author to whom correspondence should be addressed.

It is well-known that in filtration processes, particle deposition on previously deposited particles leads, over a period of time, to the eventual clogging of the filter bed. In addition, when electrical forces are involved the transient phenomena may be pronounced on a much shorter time-scale. For example, the natural charge build-up in a fluidized bed filter can be quickly neutralized by the deposition of oppositely charged particles[8]. In particle agglomeration and coating processes, the transient behavior is obviously critical to the final product characteristics. Thus, the unsteady-state behavior of particle deposition on collecting surfaces is an important problem, and one which has stimulated much work in recent years.

By far the most significant advances toward a better understanding of the transient behavior of aerosol deposition have been in the consideration of particle deposition on previously deposited particles. Various approaches to particle–particle deposition phenomena have been suggested, which include analytical methods and stochastic simulation techniques. The analytical methodology was first proposed by Payatakes and Tien[9], and was later extended in a series of papers as recently reviewed by Payatakes and Okuyama[11].

The stochastic simulation procedure, which is employed in this study, was first introduced by Tien *et al.*[10] in which particle chain formations, or dendrites, from particle–particle interception effects, were first theoretically predicted. This technique is ideal for studying complex problems in which analytical expressions are difficult to develop. For example, Nielsen and Hill[12] used the stochastic simulation procedure of Tien *et al.* and, in addition, considered the Coulombic forces between a charged particle and a charged collector. In a recent work of Auzerais

et al.[13], the two-dimensional nature of the previous studies were criticized and extensions to three dimensions made. In addition, those authors considered the presense of an electric field; however, they neglected particle inertial effects. Beizaie[4] accounted for the particle inertia through the use of curve-fitted expressions for the particle trajectories, but neglected electrical effects in the deposition calculations. In the case of many filtration systems, it has been shown that both electrical and inertial effects can be important in the analysis of the single collector efficiencies[5].

Although the results of the above cited studies clearly show the pronounced effect of particle–particle deposition, there is a lack of a general treatment of the phenomena. Furthermore, the computer calculations upon which the stochastic simulation procedures are based can be complex, and many subtleties are often involved: this is particularly true in three dimensions.

In this paper a greatly simplified method is outlined for the prediction of three dimensional, unsteady-state particle deposition on a spherical collector, taking into consideration inertial, electrostatic, drag and gravitational forces. As an example, we treat the important problem of the charge neutralization of a collecting sphere by the deposition of oppositely charged particles.

Throughout this study we consider only the case of a single spherical collector located in an infinite medium, and restrict the particle diameter to be greater than approximately 1 μm. The latter assumption means that we may neglect the Brownian motion of the particle. Extensions of the present work to multicollectors and Brownian particles may be found in Refs. [15] and [19].

THEORETICAL CONSIDERATIONS

The theoretical considerations upon which the present analysis is based begin with the equation of motion for a single particle. Applying Newton's second law of motion to the particle in an axisymmetric spherical coordinate system, as shown in Fig. 1, and using the appropriate expressions for the various forces, namely, drag, gravitational and electrostatic forces (see, e.g. Beizaie and Tien[16]), we obtain

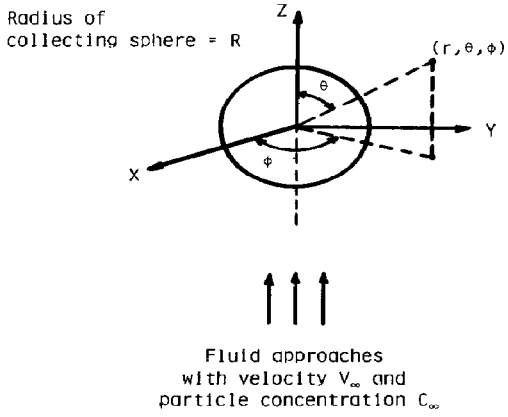

Fig. 1. Coordinate system employed in the present study.

for the r-direction

$$-\frac{\pi\rho_p d_p^3}{6}\left(1-\frac{\rho_a}{\rho_p}\right)g\cos\theta+\frac{q_p q_c}{4\pi\epsilon_0\kappa r^2}+\frac{3\pi\mu d_p}{C_s}\times\left(V_r-\frac{dr}{dt}\right)-\frac{\pi\rho_p d_p^3}{6}\left[\frac{d^2r}{dt^2}-r\left(\frac{d\theta}{dt}\right)^2\right]=0 \quad (1)$$

for the θ-direction

$$\frac{\pi\rho_p d_p^3}{6}\left(1-\frac{\rho_a}{\rho_p}\right)g\sin\theta+\frac{3\pi\mu d_p}{C_s}\left(V_\theta-r\frac{d\theta}{dt}\right)-\frac{\pi\rho_p d_p^3}{6}\left[r\frac{d^2\theta}{dt^2}+2\frac{dr}{dt}\frac{d\theta}{dt}\right]=0. \quad (2)$$

Note from eqn (1) that a uniform distribution of surface charge on the collector and a point charge on the particle has been assumed.

Introducing the following dimensionsless variables,

$$r^*=\frac{r}{R} \quad (3)$$

$$t^*=\frac{V_\infty t}{R} \quad (4)$$

$$V^*=\frac{V}{V_\infty}. \quad (5)$$

Equations (1) and (2) are transformed as,

for the r-direction

$$N_{St}\frac{d^2r^*}{dt^{*2}}+\frac{dr^*}{dt^*}-N_{St}r^*\left(\frac{d\theta}{dt^*}\right)^2-V_r^*+N_G\cos\theta-\frac{K_c}{r^{*2}}=0 \quad (6)$$

for the θ-direction

$$N_{St}\frac{d^2\theta}{dt^{*2}}+\frac{d\theta}{dt^*}+\frac{2N_{st}}{r^*}\frac{dr^*}{dt^*}\times\frac{d\theta}{dt^*}-\frac{V_\theta^*}{r^*}-\frac{N_G}{r^*}\sin\theta=0 \quad (7)$$

where,

$$N_{St}=\frac{C_s\rho_p V_\infty d_p^2}{18\mu R} \quad (8)$$

$$N_G=\frac{C_s(\rho_p-\rho_a)g d_p^2}{18\mu V_\infty} \quad (9)$$

$$K_c=\frac{C_s d_p Q_p Q_c}{3\epsilon_0\kappa\mu V_\infty}. \quad (10)$$

In the analysis it is assumed that the fluid field is known *a priori*. We have considered potential flow here, although the trajectory equations could be easily modified to consider any given flow field. The relevant expressions for the potential flow field in spherical coordinates are

$$V_r = V_\infty\left(1 - \frac{R^3}{r^3}\right)\cos\theta \tag{11}$$

$$V_\theta = -V_\infty\left(1 + \frac{R^3}{2r^3}\right)\sin\theta. \tag{12}$$

Introducing the dimensionless variables mentioned earlier, eqns (11) and (12) become

$$V_r^* = \left(1 - \frac{1}{r^{*3}}\right)\cos\theta \tag{13}$$

$$V_\theta^* = -\left(1 + \frac{1}{2r^{*3}}\right)\sin\theta. \tag{14}$$

Equations (6) and (7) were solved numerically, utilizing a 4th order Runge–Kutta method, to determine the trajectory of a single particle.

In order to study the transient behavior of particle deposition onto the collector surface a stochastic simulation technique is employed based on the principles proposed by Tien *et al.*[10]. As reviewed by Beizaie[14], the Tien *et al.* methodology is based on two important concepts associated with the deposition process, namely: (1) the increase in the total collecting area due to deposited particles; and (2) the randomness of the initial particle position in the fluid stream. The former concept is also called the shadowing effect[10] and involves the deposition of a particle on previously deposited particles. The latter concept is due to the fact that while the particle concentration in a suspension may be macroscopically uniform, the instantaneous position of any individual particle in a control surface perpendicular to the direction of flow is random. As in the Tien *et al.* methodology, a uniform random number generator is employed to simulate the initial positions for a suspension flowing toward a sphere. In addition, a control volume must be selected, as discussed by Beizaie[14], in which all possible collectable particles are considered. The sphere is located at the center and the initial particle position grid is located upstream, as shown in Fig. 2. In the present technique for simulating particle–particle deposition phenomena, the entire control volume is divided into cubical elements the size of which is equal to the diameter of the particle, that is

$$\Delta x = \Delta y = \Delta z = d_p. \tag{15}$$

For the initial position grid, the total number of possible particle positions, n, is assumed to be given by

$$n = \frac{S}{\Delta x} = \frac{S}{\Delta y} = \frac{S}{\Delta z} = \frac{S}{d_p} \tag{16}$$

where S is the total area of the grid.

Thus, a given number assigns a particle to a cube adjacent to the initial position grid as shown in Fig. 2. Although the initial particle position could be, theoretically, anywhere along the grid and not restricted to a finite number of positions, the work of Beizaie[14] suggests that such an approximation should be valid as long as the ratio of particle size to collector size is small.

Once a particle position has been selected by a suitable random number generator, its trajectory is followed as it moves through the 3-D grid composed of the cubical elements. The collecting sphere itself is approximated by the cubical elements; its volume is therefore given by

$$V_{\text{sphere}} = \sum_{KC-L}^{KC+L}\sum_{JC-M}^{JC+M}\sum_{IC-N}^{IC+N}\Delta x\Delta y\Delta z \tag{17}$$

where IC, JC and KC are the coordinates of the center of the sphere and

$$N = \frac{R}{\Delta x} \tag{18}$$

$$M = \frac{(R^2 - x^2)^{1/2}}{\Delta y} \tag{19}$$

$$L = \frac{(R^2 - x^2 - y^2)^{1/2}}{\Delta z}. \tag{20}$$

Over each differential time a determination is made as to which cubical element the particle lies by the

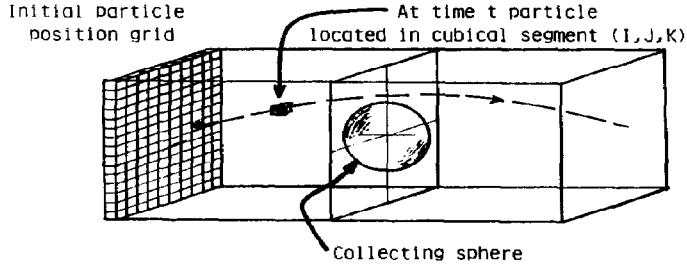

Fig. 2. Illustration of the control volume and a typical particle trajectory.

following equations

$$I = \frac{x}{d_p} + IC \tag{21}$$

$$J = \frac{y}{d_p} + JC \tag{22}$$

$$K = \frac{z}{d_p} + KC \tag{23}$$

where x, y and z are the present cartesian coordinates of the particle position.

A testing procedure is then invoked to determine if the cube in which the particle lies is adjacent to any cubical elements of the sphere (primary collection), or, a cubical element occupied by a deposited particle (secondary collection).

The testing procedure can be made quite simple by coding each cube in the control volume. For example, a code number of one indicates an empty cube; a code number of two indicates a cube occupied by a deposited particle; and a code number of three indicates a cubical segment of the sphere.

If the cube in which the particle lies is adjacent to either a cube with code 2 or 3, the trajectory analysis for that particle is stopped and that position in the grid is permanently assigned the code 2. If any particle moving in the control volume is not collected within its boundaries, it is considered to have escaped and the trajectory analysis for that particle is stopped.

Because the possibility of particle–particle interactions exists, for example, electrical attractions and repulsions, it is necessary to consider the simultaneous motion of all particles within the control volume at a given time. Although we will not consider particle–particle interaction forces here (except for the collector charge neutralization phenomenon presented later in this paper), we will nonetheless consider the simultaneous particle motions.

In general, there are two time steps in the simulation which must be considered. The first time step is necessary for the stable and accurate numerical integration of eqns (6) and (7). The second time step, or interval, is the duration between successive particle generations at the initial position surface. This time interval is related to the particle number flux as

$$t = \frac{1}{V_\infty C_\infty S} \tag{24}$$

where V_∞ is the free stream fluid velocity and C_∞ is the bulk freestream number concentration of particles.

Thus, over each time interval given by eqn (24) a particle is generated at the initial surface with its position selected according to the uniform random number generator employed. The positions of all of the particles within the control volume are followed in time until they have either deposited or escaped.

The testing procedure as described above is deficient in one aspect, namely, that the particle position center may not be at the exact center of the cubical element determined by eqns (21)–(23). Therefore, the testing procedure should only be invoked on the surrounding cubes in which particle–particle deposition is physically possible. This is easily accomplished using a simple "rule-out" procedure prior to the actual test.

Finally, we note that additional assumptions made in the present analysis include: (1) changes in the flow field around the collector due to deposited particles are neglected; (2) the system under consideration is

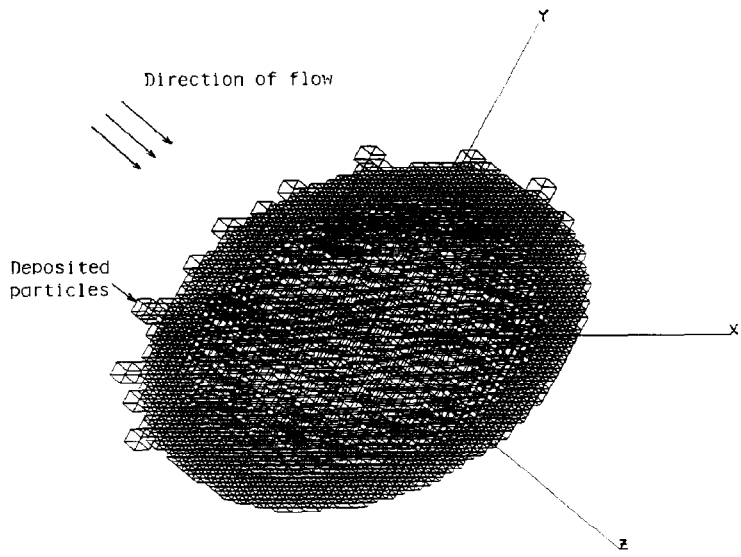

Fig. 3. Real-time simulation of particle deposition in the absence of electrostatic forces. The values of the input parameters are given in Table 1.

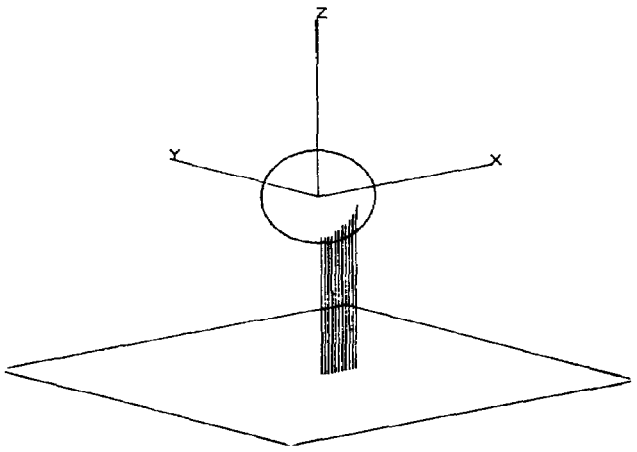

Fig. 4. Typical particle trajectories in the absence of electrostatic forces corresponding to Fig. 3.

isothermal, and the fluid is incompressible; and (3) the effect of re-entrainment of particles once they are collected, due to the imbalancing of shear and adhesive forces, has been neglected.

In the simulation studies presented here the control volume was selected large enough such that no particle outside the initial position grid had the possibility of being collected. In addition, to conserve storage space, the initial position grid was located four collector radii upstream. This will introduce small errors in utilizing the infinite medium expressions of eqns (11) and (12)[16]. However, in a practical application of the theory to the multicollector case, the control volume would be selected on the basis of the voidage (for example via a unit cell type model[17]), and the ambiguities mentioned above would disappear (also, see the discussion in Ref. [15]).

RESULTS AND DISCUSSION

Typical simulation results utilizing the proposed methodology are shown in Figs. 3–10. The dynamic calculations were limited to approximately 400 particles in total. Figure 3 shows a three dimensional plot illustrating particle deposition on a spherical collector considering the effect of gravity, drag and inertia only. The values of the input parameters corresponding to Fig. 3 are given in Table 1. Note that the plots are conveniently made by drawing only the surface cubes of the collecting sphere (part of the code 3 cubes) and all deposited particle cubes (code 2 cubes). It is evident from Fig. 3 that the deposition of particles under the absence of electrostatic forces takes place only on the front half of the sphere, in the direction of flow. This result is expected from plotting typical particle trajectories for the system of Fig. 3, as shown in Fig. 4.

In Fig. 5 the electrostatic force term is added to the equations of motion and collection of particles around the entire sphere is now observed (refer to Table 2 for the values of the input parameters for this case). The results in Fig. 5 are again expected from plotting the particle trajectories with the inclusion of the electrostatic force as shown in Fig. 6. Note that the effect of charge neutralization of the collecting sphere due to the deposition of oppositely charged particles is not included in Fig. 6.

The total number of particles collected as a function of time corresponding to Figs. 3 and 4 are shown in Figs. 7 and 8, respectively. As noted by Beizaie[14], the chaotic nature of the plots is due to the random positions of the particles being considered. However, the present results show that under the conditions of large electrostatic forces the chaotic nature begins to disappear, since the initial particle position becomes less important. Note also from Figs. 7 and 8 the

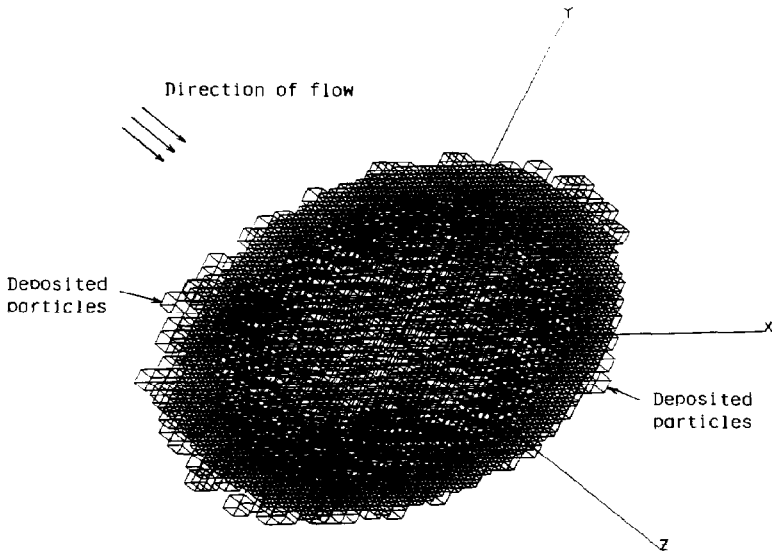

Fig. 5. Real-time simulation of particle deposition with the inclusion of electrostatic forces. The values of the input parameters are given in Table 2.

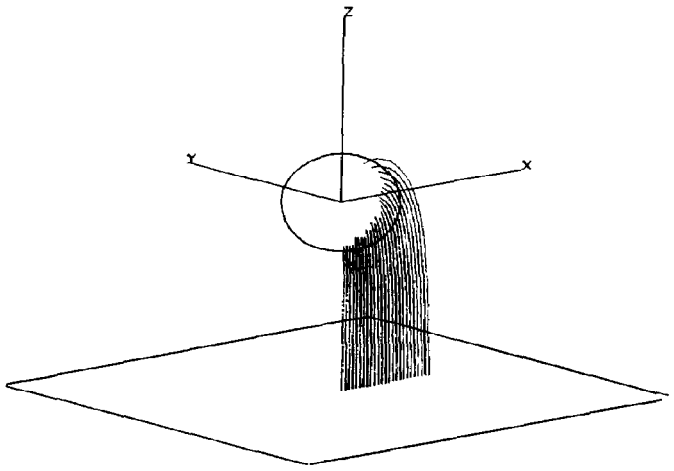

Fig. 6. Typical particle trajectories with the inclusion of electrostatic forces corresponding to Fig. 5.

differences in the magnitude of particles collected as a function of time. For example, at time $t = 0.04$ sec only 10 particles were collected when the Stokes number was high and electrostatic forces absent; however, during the same time 75 particles were collected when electrostatic forces were present and the Stokes number was small.

Although the above results illustrate the dynamic behavior by following the number of particles deposited as a function of time, in order to compare to previously given deposition calculations, the results should be expressed in terms of the single collector efficiencies.

Use of the aerosol dynamics simulation for determining the single collector efficiencies

As a check of the computational scheme developed, some simulations were conducted to determine the limiting particle deposition trajectories. These were obtained in the usual fashion[6] with particle–particle deposition ignored.

In Fig. 9 the results for the combined case of inertial and electrostatic forces are compared to the sum of the expressions for inertial deposition[6] and electrostatic deposition[18]. This technique is known

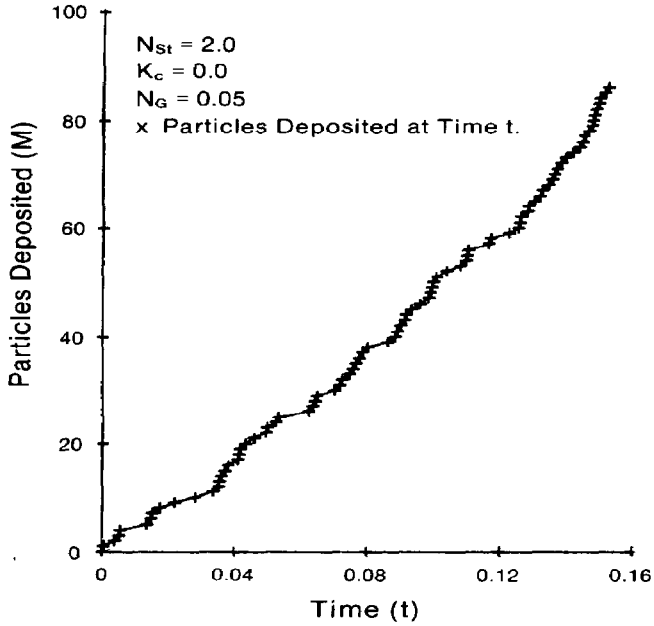

Fig. 7. Number of particles collected as a function of time corresponding to Fig. 3.

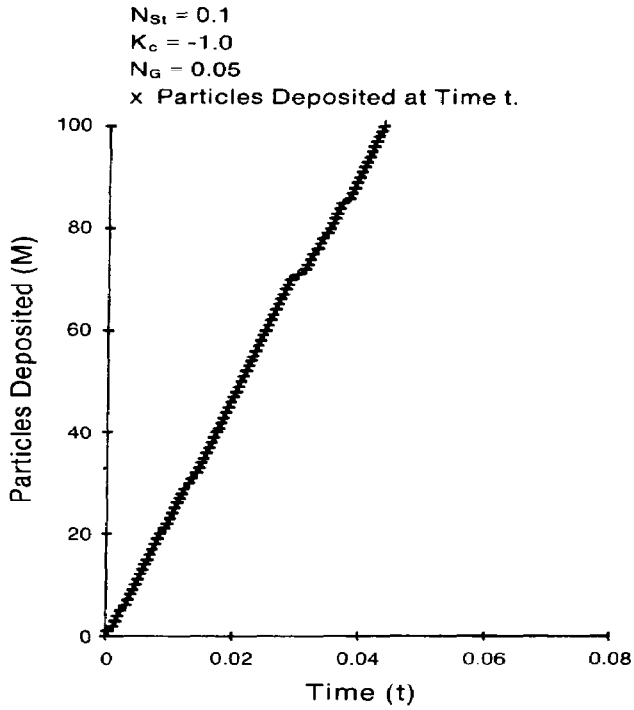

Fig. 8. Number of particles collected as a function of time corresponding to Fig. 5.

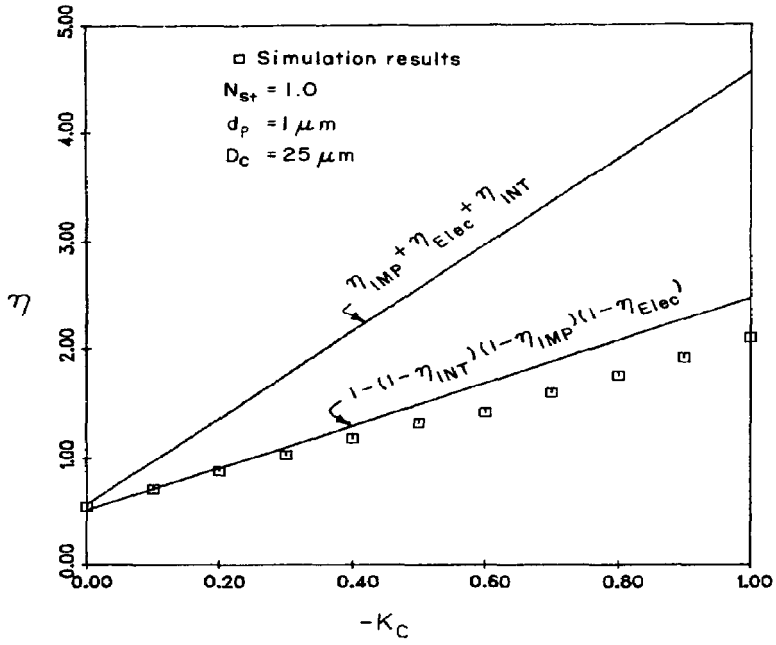

Fig. 9. Comparison of the calculated clean collector efficiencies to previously reported results[6, 18].

as the principle of superposition, and it is clearly invalid for this type of system. A simple physical explanation is that the presence or absence of inertial forces makes little difference to the particle trajectories which result in collection by attractive electrostatic forces.

From a probability point of view, the mechanisms of particle deposition in Fig. 9 are better regarded as independent events; thus

$$\eta = 1 - [(1 - \eta_{INT})(1 - \eta_{IMP})(1 - \eta_{EI})]. \quad (25)$$

As shown in Fig. 9, eqn (25) is in excellent agreement with the calculated values, except at large values of the electrostatic force. When K_c assumes large negative values with $\eta > 1$, particle collection takes place on the backside of the collector where the inertial force opposes the electrical attractive force; thus, eqn (25) would not be expected to hold.

Although the above results show some interesting features of the clean collector efficiency, the major emphasis in this work is on the prediction of the transient behavior of aerosol deposition. The single collector efficiency in this case can be expressed in terms of the change in the number of particles deposited as a function of time, as

$$\eta(t) = \frac{1}{\pi R^2 V_\infty C_\infty}\left(\frac{dM}{dt}\right). \quad (26)$$

As an illustration, some simulations for the case of attractive electrostatic forces, with inertial and gravitational forces, were carried out as shown in Fig. 10. The time dependent collector efficiencies were calculated according to eqn (26), replacing the differential by $\Delta M/\Delta t$, and selecting a time interval over which an appreciable change in ΔM would occur (0.2 sec in Fig. 10).

Two cases were considered in obtaining the results shown in Fig. 10. In the first case, the change in the net attractive force due to the deposition of oppositely charged particles is neglected. The single collector efficiency under this condition is shown to steadily increase with time, passing through and eventually exceeding the initial, or clean, collector efficiency value, as shown by the solid line.

If, on the other hand, we account for the neutralization of segments of the collecting sphere surface by the deposition of oppositely charged particles we obtain the dramatic result shown in Fig. 10. Here, the net electrostatic force that any particle approaching the collecting sphere experiences is simply computed by first summing the repulsive forces between the approaching particle and any previously deposited particles (code 2 cubes); this value is then subtracted from the attractive force computed for the "clean" collecting sphere. Thus, the repulsive force contribution must be determined each time the particle is moved. Note that we have assumed that the initial charges on the sphere are bound charges, as in an insulator. In any event, the rapid drop in the single collector efficiency with time shown in Fig. 10, indicates the potential importance of charge neutralization phenomena, as well as the versatility of the present computational scheme in accounting for such effects. Certainly experimental verification of the results given here is warranted for future investigations.

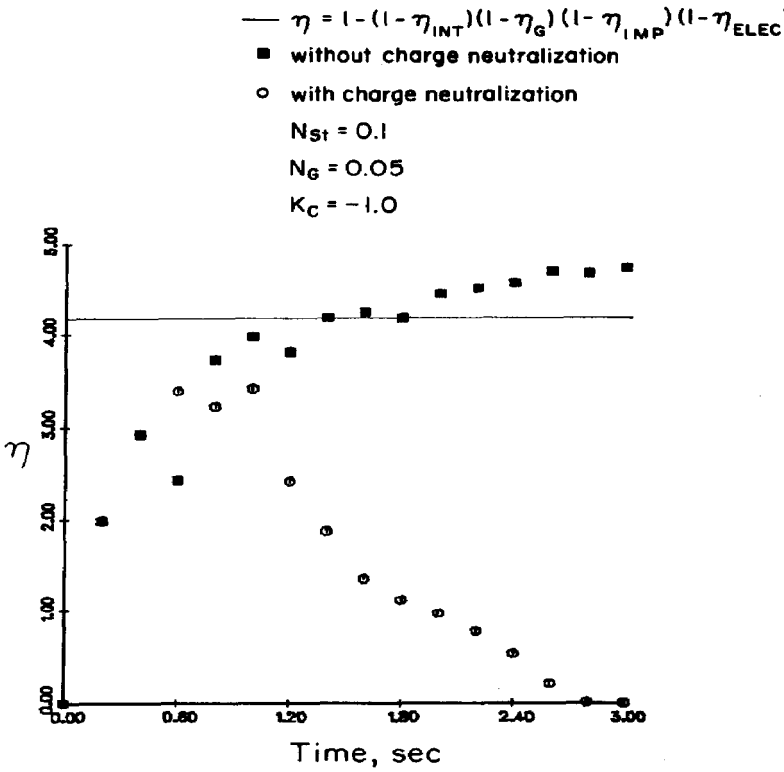

Fig. 10. Calculated time dependent collection efficiencies with and without charge neutralization effects.

CONCLUSIONS

A thorough analysis of particle deposition onto collecting surfaces requires the consideration of the time-dependent phenomena of particle build-up, adhesion and re-entrainment.

In the present work, a theoretical approach to the prediction of particle–particle deposition phenomena (time-dependent particle build-up) on a spherical collector is given based on a discretization of the surrounding control volume into cubical elements. Several particle deposition problems are selected to exemplify the ease with which the control volume discretization technique can accommodate a variety of force term combinations.

A dramatic example considered is the charge neutralization of an initially uniformly charged sphere by the deposition of oppositely charged particles. Although the force term is time-dependent in this case, little complication is introduced into the aerosol dynamics simulation. Future work extending the concepts of this paper will involve the inclusion of Brownian motion (Brownian dynamics) and particle–particle interactions prior to any deposition[15, 19].

NOTATION

- C_c particle-slip correction factor
- C_∞ free stream particle number concentration, number of particles/cm^3
- d_p diameter of the particle, cm
- g acceleration due to gravity, cm/s^2
- I x coordinate of a particle position in the control volume

Table 1. The values of the input parameters employed in Figs. 3, 4 and 7

STOKES NUMBER, N_{St} = 2.0
ELECTROSTATIC FORCE PARAMETER, K_c = 0.0
GRAVITATIONAL NUMBER, N_G = 0.05
COLLECTOR DIAMETER, D_c = 25 micron
PARTICLE DIAMETER, d_p = 1 micron

Table 2. The values of the input parameters employed in Figs. 5, 6 and 8

STOKES NUMBER, N_{St} = 0.1
ELECTROSTATIC FORCE PARAMETER, K_c = -1.0
GRAVITATIONAL NUMBER, N_G = 0.05
COLLECTOR DIAMETER, D_c = 25 micron
PARTICLE DIAMETER, d_p = 1 micron

IC x coordinate of the sphere center
J y coordinate of a particle position in the control volume
JC y coordinate of the sphere center
K z coordinate of a particle position in the control volume
KC z coordinate of the sphere center
K_c dimensionless electrostatic parameter
M total number of collected particles
N total number of possible particle positions
N_G dimensionless gravitational number
N_{St} Stokes number
q_c charge on the collector, Coulomb
q_p charge on the particle, Coulomb
Q_c charge density on the collector, Coulomb/cm^2
Q_p charge density on the particle, Coulomb/cm^2
r radial distance, cm
r^* dimensionless radial distance, $r^* = (r/R)$
R radius of the collector, cm
S surface area of the initial particle position grid
t time, s
t^* dimensionless time, $t^* = (V_\infty t/R)$
V_r radial fluid velocity, cm/s
V_r^* dimensionless radial fluid velocity
V_θ fluid velocity in the θ-direction, cm/s
V_θ^* dimensionless fluid velocity in θ-direction
V_∞ free stream fluid velocity, cm/s
V_{sphere} volume of the sphere
Δx increment in the x direction
Δy increment in the y direction
Δz increment in the z direction

Greek symbols

κ fluid dielectric constant
ϵ_0 permitivity of free space, Coulomb^2-s^2/g-cm^3
η single collector efficiency
μ viscosity of the fluid, g/cm-s
ρ_a density of the fluid, g/cm^3
ρ_p density of the particle, g/cm^3

REFERENCES

[1] Gutfinger C. and Tardos G. I., *Atm. Environ.* 1979 **13** 853.
[2] Peters M. H., Fan L.-S. and Sweeney T. L., *A.I.Ch.E.J.* 1982 **28** 39.
[3] Pearson H. J., Puttock J. S. and Hunt J. C. R., *J. Fluid Mech.* 1983 **129** 219.
[4] Cleaver J. W. and Yates B., *Chem. Engng Sci.* 1976 **31** 147.
[5] Tien C., *Chem. Engng Commun.* 1982 **17** 361.
[6] Langmuir I., *J. Meterology* 1948 **5** 175.
[7] Emi H., Wang C. and Tien C., *A.I.Ch.E.J.* 1982 **28** 397.
[8] Tardos G., Pfeffer R., Peters M. and Sweeney T., *Ind. Engng Chem. Fundls* 1983 **22** 445.
[9] Payatakes A. C. and Tien C., *J. Aerosol Sci.* 1976 **7** 85.
[10] Tien C., Wang C. and Barot D. T., *Science* 1977 **196** 983.
[11] Payatakes A. C. and Okuyama K., *Proc. Int. Symp. on Powder Technology* 81 Kyoto, Japan 1981.
[12] Nielsen K. A. and Hill J. C., *A.I.Ch.E.J.* 1980 **26** 678.
[13] Auzerais F., Payatakes A. C. and Okuyama K., *Chem. Engng Sci.* 1983 **38** 447.
[14] Beizaie M., Ph.D. Dissertation, Syracuse University, New York 1977.
[15] Peters M. H. and Gupta D., Brownian dynamics in fixed and fluidized bed filtration. *A.I.Ch.E. Symp. Ser. on Fluidization and Fluid-Particle Systems* No. 234 1984 **80** 98.
[16] Beizaie M. and Tien C., *Can. J. Chem. Engng* 1980 **58** 12.
[17] Neale G. H. and Nader W. K., *A.I.Ch.E.J.* 1973 **19** 112.
[18] Nielsen K. A. and Hill J. C., *Ind. Engng Chem. Fundls* 1976 **15** 149.
[19] Gupta, D. and Peters M. H., A Brownian Dynamics Simulation of Aerosol Deposition onto Spherical Collectors. *J. Colloid and Interface Science* (in Press) 1984.